Submitted to ApJ Letters
Preprint typeset using LaTeX style emulateapj v. 16/07/00

THE AGE OF THE UNIVERSE AND THE COSMOLOGICAL CONSTANT DETERMINED FROM COSMIC MICROWAVE BACKGROUND ANISOTROPY MEASUREMENTS

Lloyd Knox
Department of Physics, University of California, Davis, CA 95616, USA, email: lknox@ucdavis.edu
Nelson Christensen
Physics and Astronomy, Carleton College, Northfield, MN, 55057, USA email: nchriste@carleton.edu
and
Constantinos Skordis
Department of Physics, University of California, Davis, CA 95616, USA, email: skordis@bubba.ucdavis.edu
Submitted to ApJ Letters

ABSTRACT

If $\Omega_{\rm tot} = 1$ and structure formed from adiabatic initial conditions then the age of the Universe, as constrained by measurements of the cosmic microwave background (CMB), is $t_0 = 14.0 \pm 0.5$ Gyr. The uncertainty is surprisingly small given that CMB data alone constrain neither h nor Ω_Λ significantly. It is due to the tight (and accidental) correlation, in these models, of the age with the angle subtended by the sound horizon on the last–scattering surface and thus with the well-determined acoustic peak locations. If we assume either the HST Key Project result $h = 0.72 \pm .08$ or simply that $h > 0.55$, we find $\Omega_\Lambda > 0.4$ at 95% confidence—another argument for dark energy, independent of supernovae observations. Our analysis is greatly simplified by the Monte Carlo Markov chain approach to Bayesian inference combined with a fast method for calculating angular power spectra.

Subject headings: cosmology: theory – cosmology: observation – methods: data analysis – methods: statistical – cosmology: cosmic microwave background, cosmological parameters, distance scale

1. INTRODUCTION

Determining the expansion age of the Universe has been a major goal of cosmology ever since Hubble discovered the expansion. Compatibility with determinations of stellar ages is an important consistency check of cosmological models. Traditional methods of determining the expansion age rely on Hubble constant measurements which are either highly imprecise, or have error budgets dominated by systematics. In addition one must determine Ω_Λ (or more generally the mean density of the various components) since it affects how the expansion rate has changed over time. In this *Letter* we present highly precise age determinations from CMB data which completely bypass the need for independent determinations of H_0 and Ω_Λ.

There are a handful of cosmological parameters which can be determined from measurements of the CMB angular power spectrum to percent level accuracy, such as ω_b, ω_m, and $\Omega_{\rm tot}$ (where $\omega_i \equiv \Omega_i h^2$ and $H_0 = 100h\,{\rm km\,sec^{-1}\,Mpc^{-1}}$) (e.g. Eisenstein et al. 1999). Other parameters can not be well–determined and require the addition of complementary observations. For example Ω_Λ is poorly determined by the CMB alone(e.g. Efstathiou & Bond 1999) but well–determined when supernovae observations are included (e.g. Netterfield et al. 2001).

It has been pointed out (Ferreras et al. 2001) and demonstrated (Netterfield et al. 2001) that the CMB can be used to place tight constraints on the age of the Universe. This is due to the high degree of correlation between the angle subtended by the sound–horizon on the last–scattering surface, θ_s, and age in flat adiabatic models, also noticed by Hu et al. (2001) who used it to place an *upper* bound on the age. Here we extend the previous work by including additional data, by taking the flatness assumption seriously and by use of a new analysis technique which has advantages as described below. We also demonstrate the accidental nature of the age–sound horizon correlation by showing that its tightness depends on where we are in the Ω_Λ, h parameter space. We are fortunate that the correlation is tightest near the "concordance" values of $h = 0.72$ and $\Omega_\Lambda = 0.65$.

Our age determination is model–dependent and the model (adiabatic CDM) has many parameters. We take them to be the amplitude and power–law spectral index of the primordial matter power spectrum, A and n, the baryon and dark matter densities, ω_b and ω_d, the cosmological constant divided by the critical density, Ω_Λ, and the redshift of re-ionization of the intergalactic medium, $z_{\rm ri}$. The Hubble constant and age are derived parameters, given in terms of the others by $h^2 = (\omega_b + \omega_d)/(1 - \Omega_\Lambda)$ and $t_0 = 6.52$ Gyr $\ln[(1 + \sqrt{\Omega_\Lambda})/\sqrt{1 - \Omega_\Lambda}]/\sqrt{\Omega_\Lambda h^2}$.

We do not consider models with $\Omega_{\rm tot} \neq 1$ or dark energy models other than the limiting case of a cosmological constant with $w \equiv P/\rho = -1$. The first we justify on grounds of simplicity: CMB observations indicate the mean curvature is close to zero and generally agree well with inflation. If we did allow the curvature to vary, our age result would become significantly less precise. We expect allowing w to vary to have little effect, as we discuss below.

We explore the likelihood in a ten–dimensional parameter space (six cosmological parameters plus four experimental parameters) by Monte–Carlo generation of a Markov chain of parameter values as described in Christensen et al. (2001). From the chain one can rapidly calculate marginalized one–dimensional or two–dimensional probability distributions for chain parameters, or derived parameters, with or without additional priors. Generating a sufficiently long chain in a reasonable amount of time requires a fast means of calculating the angular power spec-

trum for a given model. We describe this fast method briefly below and more thoroughly in Kaplinghat et al. (2001).

Supernovae observations constrain the combination $H_0 t_0$ better than either parameter by itself. Perlmutter et al. (1999) find for flat Universes that $t_0 = 13.0^{+1.2}_{-1.0}(0.72/h)$ Gyr. Combining this result with our t_0 determination leads to $h = 0.67^{+.07}_{-.06}$, in agreement with the HST result. Riess et al. (1998) find for arbitrary $\Omega_{\rm tot}$ that $t_0 = (14.2 \pm 1.7)$ Gyr.

Krauss & Chaboyer (2001) estimate the age of 17 metal–poor globular clusters to be $t_{\rm GC} = 12.5$ Gyr with a 95% lower bound of 10.5 Gyr and a 68% upper bound of 14.4 Gyr. The minimum requirement for consistency, that $t_f \equiv t_0 - t_{\rm GC} > 0$ is easily satisfied with a few Gyrs to spare. Unfortunately, the upper bound on $t_{\rm GC}$ is not sufficiently restrictive to set an interesting lower bound on t_f.

Below we tabulate our constraints on all the model parameters, and emphasize not only t_0 but also Ω_Λ. With the inclusion of prior information on H_0, the CMB data provide strong evidence for $\Omega_\Lambda > 0$. The same conclusion can be reached by, instead, combining the CMB data with observations of large–scale structure (Efstathiou et al. 2001) or clusters of galaxies (Dodelson & Knox 2000).

2. METHOD

Our first step in exploring the high–dimensional parameter space is the creation of an array of parameter values called a chain, where each element of the array, $\vec{\theta}$, is a location in the n-dimensional parameter space. The chain has the useful property once it has converged that $P(\vec{\theta} \in R) = N(\vec{\theta} \in R)/N$ where the left–hand side is the posterior probability that $\vec{\theta}$ is in the region R, N is the total number of chain elements and $N(\vec{\theta} \in R)$ is the number of chain elements with $\vec{\theta}$ in the region R. Once the chain is generated one can then rapidly explore one–dimensional or two–dimensional marginalizations in either the original parameters, or in derived parameters, such as t_0. Calculating the marginalized posterior distributions is simply a matter of histogramming the chain.

2.1. *Generating the Chain*

The chain we generate is a Monte Carlo Markov Chain (MCMC) produced via the Metropolis–Hastings algorithm described in Christensen et al. (2001). The candidate–generating function for an initial run was a normal distribution for each parameter. Subsequent runs used a multivariate–normal distribution with cross–correlations between cosmological parameters equal to those of the posterior as calculated from the initial run.

All of our results are based on MCMC runs consisting of 2×10^5 iterations. For the "burn-in" the initial 2.5×10^4 samples were discarded, and the remaining set was thinned by accepting every 25th iteration. We used the CODA software (Best et al. 1995) to confirm that all chains passed the Referty-Lewis convergence diagnostics and the Heidelberger-Welch stationarity test.

While generating the chain we always restrict our sampling to the $h > 0.4$ and $5.8 < z_{\rm ri} < 6.3$ region of parameter space. The former is a very conservative lower–bound on h and the latter is a simple interpretation of the spectra of quasars at very high redshift (Becker et al. 2001; Djorgovski et al. 2001). For some of our results we assume an "HST prior" which means $h = 0.72 \pm 0.08$ (Freedman et al. 2001) with a normal distribution.

2.2. *C_l Calculation*

We calculate C_l rapidly with a preliminary version of the Davis Anisotropy Shortcut (DASh; Kaplinghat et al. 2001). We first calculate the Fourier and Legendre–transformed photon temperature perturbation, $\Delta_l(k)$, on a grid over parameters ω_b and ω_d at fixed values of $\Omega_k \equiv 1 - \Omega_{\rm tot} = \Omega_k^*$, $\Omega_\Lambda = \Omega_\Lambda^*$ and $\tau = 0$ using CMBfast (Seljak & Zaldarriaga 1996). From this grid, we get C_l for any ω_b, ω_d, and the primordial power spectrum $P(k) = A(k/0.05 Mpc^{-1})^n$ by performing multi–linear interpolation on the grid of $\Delta_l(k)$ and then the following integral:

$$\mathcal{C}_l \equiv \frac{l(l+1)C_l}{2\pi} = 8\pi l(l+1) \int k^2 dk \Delta_l^2(k) P(k). \qquad (1)$$

We can get any C_l in the entire model space of $\{\omega_b, \omega_d, \tau, \Omega_\Lambda, \Omega_k, P(k)\}$ by the use of analytic relations between the $\Delta_l(k)$ for different models. For varying Ω_Λ and Ω_k, $\mathcal{C}_l = \mathcal{C}_{\tilde{l}}$ where $l/\tilde{l} = \theta_s(\Omega_k^*, \Omega_\Lambda^*)/\theta_s(\Omega_k, \Omega_\Lambda)$ and θ_s is the angle subtended by the sound–horizon at the last–scattering surface. For $\Omega_k = 0$, $\theta_s = s/\eta_0$ where η_0 is the conformal time today (or, equivalently, the comoving distance to the horizon) and s is the comoving sound–horizon at the last–scattering surface.

Altering θ_s is not the only effect of varying Ω_k and Ω_Λ. Varying Ω_k changes the eigenvalues of the Laplacian on very large scales and hence the power spectrum at the last–scattering surface, and both Ω_k and Ω_Λ affect the late–time evolution of the gravitational potential. Both of these effects only affect C_l at $l << 100$. We therefore make an additional grid over the parameters ω_b, ω_d, Ω_k and Ω_Λ but with smaller maximum l and k values than the lower–dimensional high-l grid. The low-l grid used for the calculations presented here has ranges $0.01 < \omega_b < 0.03$, $0.05 < \omega_d < 0.25$, and $0 < \Omega_\Lambda < 0.85$ with 4, 4, and 8 uniformly spaced samplings of the range respectively. For the present application we have fixed $\Omega_k = 0$. For the high-l grid the ranges for ω_b and ω_d are the same but with twice as many samples, and $\Omega_\Lambda^* = 0.6$.

The split into a low-l grid and a high-l grid has been used by others, although for grids of C_l, not $\Delta_l(k)$. We follow Tegmark et al. (2001) in joining our grids with a smooth k-space kernel, $g(k) = 2/(1 + exp(2k/k_s)^4)$ where $k_s = 1.5/s$; in the integrand of Eq. 1 $P(k)$ is replaced with $g(k)P(k)$ for the low-l grid and $(1 - g(k))P(k)$ for the high-l grid and $C_l = C_l^{\rm low} + C_l^{\rm high}$. Finally, we allow for non-zero z_{ri} by sending $C_l \to \mathcal{R}_l(z_{ri})C_l$ where $\mathcal{R}_l(z_{ri})$ is given by the fitting formula of Hu & White (1996).

2.3. *Likelihood Calculation*

To calculate the likelihood we use the offset log-normal approximation of Bond et al. (2001) which is a better approximation to the likelihood function than a normal distribution. We include bandpower data from Boomerang, the Degree Angular Scale Interferometer (DASI; Halverson et al. 2001), Maxima (Lee et al. 2001)) and the COsmic Background Explorer(COBE; Bennet et al. 1996). The weight matrices, band powers and window functions for

DASI are available in Leitch et al. (2001), Halverson et al. (2001) and Pryke et al. (2001). For COBE we approximate the window functions as tophat bands; all other information is available in Bond et al. (2001) and in electronic form at RadPack (2001). For Boomerang and Maxima we approximate the window functions as top-hat bands, the weight matrices as diagonal and the log-normal offsets, x, as zero. The Boomerang team report the uncertainty in their beam full-width at half-maximum (fwhm) as 12.9 ± 1.4 minutes of arc. We follow them in modelling the departure from the nominal (non-Gaussian) beam shape as a Gaussian. For the Boomerang $Z_i^t, \mathcal{C}_l$ is therefore actually $\mathcal{C}_l \exp(-l^2 b^2)$. Our prior for b is uniform, bounded such that the fwhm is always between 11.5' and 14.3'. Calibration parameters, for example, $u_{\rm DASI} = 1 \pm 0.04$ are taken to have normal prior distributions and alter model angular power spectra via $C_l \to u^2_{\rm DASI} C_l$ prior to comparison with the reported band powers. To reduce our sensitivity to beam errors, we only use bands with maximum l-values less than 1000. Thus we use all nine DASI bands, the first 11 Maxima bands and all but the last Boomerang band.

Five of the 24 DASI fields are completely within the area of sky analyzed by Boomerang, and three partially overlap this area. We expect the resulting DASI–Boomerang bandpower error correlations (which we neglect) to be small and to have negligible effect on our results.

3. RESULTS

In the top panel of Figure 1 we see that neither h nor Ω_Λ can be constrained well by CMB data alone. The shape of the contour "banana" in the top panel is determined by the dependence of the well–determined θ_s on h and Ω_Λ; lines of constant θ_s run along the ridge of high likelihood. Since θ_s correlates well with the age, as seen in Fig. 2, the ridge of high likelihood is also at nearly constant age.

Although Ω_Λ is poorly determined by CMB data alone we find that addition of the HST prior allows one to set a 95% lower limit of $\Omega_\Lambda > 0.4$. This same lower bound can be achieved by simply rejecting models with $h < 0.55$.

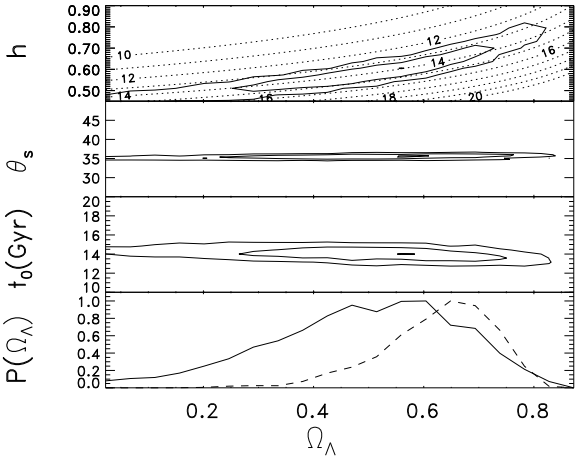

FIG. 1.— The posterior probability density of Ω_Λ (lowest panel) and contours of equal probability density in the Ω_Λ, t_0 plane (lower middle panel), Ω_Λ, θ_s plane (upper middle panel) and Ω_Λ, h plane (top panel). Contour levels are at $e^{-6.17/2}$, $e^{-2.3/2}$ and 0.95 of maximum. The lowest panel curves are for $h > 0.4$ (solid) and $h = .72 \pm .08$ (dashed). Top panel dotted lines are at constant t_0.

We can understand the $t_0 - -\theta_s$ correlation with the aid of an approximate analytic expression given by Hu et al. (2001) from which we derive

$$\frac{\Delta\theta_s}{\theta_s} = 0.060(2.9\frac{\Delta\omega_m}{\omega_m} + 1.0\frac{\Delta\omega_\Lambda}{\omega_\Lambda} - 1.14\frac{\Delta\omega_b}{\omega_b}) \quad (2)$$

for the fiducial values $\omega_m = 0.15, \omega_\Lambda = 0.3, \omega_b = 0.02$. Expanding t_0 about our fiducial values we find

$$\frac{\Delta t_0}{t_0} = -0.12\left(3.0\frac{\Delta\omega_m}{\omega_m} + 1.2\frac{\Delta\omega_\Lambda}{\omega_\Lambda}\right). \quad (3)$$

Thus a change from the fiducial values by $\Delta\omega_m$ and $\Delta\omega_\Lambda$ which keeps θ_s fixed will nearly leave the age unchanged.

In general, the parameter controlling this correlation is the ratio of ratios:

$$R = \frac{(\partial \ln\theta_s/\partial\ln\omega_m)/(\partial\ln\theta_s/\partial\ln\omega_\Lambda)}{(\partial\ln t_0/\partial\ln\omega_m)/(\partial\ln t_0/\partial\ln\omega_\Lambda)} \quad (4)$$

and the correlation is tightest when $R = 1$. R has little dependence on ω_b. For what used to be called standard CDM, $R = 0.75$. R can be as small as 0.53 for $\Omega_m = 1$ and $h = 0.72$ and as large as 2.0 for $\Omega_\Lambda = 0.83$ and $h = 0.72$. At the maximum of the likelihood, $R = 0.88(1.08)$ with (without) the HST prior.

As a test, we have estimated the age via a direct grid–based evaluation of the likelihood given DASI and DMR data using CAMB (Lewis et al. 2000) to calculate C_l's. Taking the grid parameters to be t_0, ω_d, n and A and fixing $u_{\rm DASI} - 1 = \omega_b - 1 = \Omega_k = z_{\rm ri} = 0$ we find $t_0 = (13.6 \pm 0.6)$ Gyr. This agrees very well with our MCMC + DASh results when the same assumptions and data selection are made: $t_0 = (13.7 \pm 0.6)$ Gyr. We can also reproduce the Netterfield et al. (2001) result, finding for Boomerang and DMR data (although ignoring the highest–l Boomerang bandpower) $t_0 = (14.32 \pm 0.68)$ Gyr.

In the table we show means and standard deviations for our ten original parameters and a number of derived parameters. Particularly noteworthy is θ_s, determined with an error of less than 3%. The agreement between the datasets on this number is also remarkable. From DASI $\theta_s = (0.60 \pm 0.01)$ degrees and from Boomerang $\theta_s = (0.59 \pm 0.01)$ degrees.

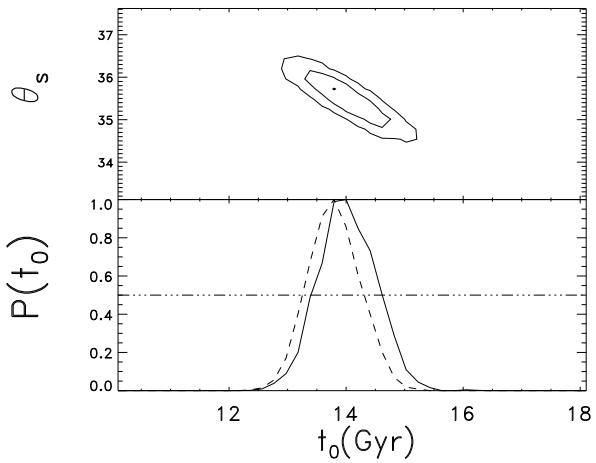

FIG. 2.— The posterior probability density of the age of the Universe (lower panel) and contours of equal probability density (as in Figure 1) in the θ_s, t_0 plane (upper panel). The lower panel curves are for $h > 0.4$ (solid) and $h = .72 \pm .08$.

For studying the early evolution of structure, it is useful to know the age at redshifts in the matter–dominated era. For $1 << z < 100$, $t_z \times (1+z)^{3/2} = 6.52/\sqrt{\omega_m}$ Gyr $= (16 \pm 1)$ Gyr, where t_z is the age at redshift z. Since *MAP*[1] and *Planck*[2] will determine ω_m to 10% and 2% respectively (Eisenstein et al. 1999) they will determine $t_z \times (1+z)^{3/2}$ to 5% and 1% respectively.

4. DISCUSSION

Since our argument is model–dependent, it is worth pointing out that the model has been enormously successful on the relevant length scales (e.g. Wang et al. 2001). Perhaps the weakest link is the dark energy equation of state since we have scant guidance from observations (e.g. Perlmutter et al. 1999) and even less from theory. Fortunately, one can show that varying the equation of state away from $w = -1$ at fixed θ_s has very little effect on the age: at $\theta_s = 0.6$ degrees and $\omega_m = 1/3$, $\Delta t_0/t_0 = .05\Delta w$. Though we neglect the possibility of gravitational wave contributions to C_l (see Efstathiou 2001) we do not expect these to make much difference since θ_s is relatively unaffected by measurements at low ℓ where gravitational waves are important.

Our age determination has the benefit of being derived from observations whose statistical properties can be predicted highly accurately using linear perturbation theory. We are encouraged that the observational errors are dominated by the reported statistical ones since nearly the same result can be derived from two independent data sets. We conclude that the best determination of t_0 now comes from CMB data. The prospects for improving the age determination are bright since the statistical errors (and any systematic ones too) will be greatly reduced by *MAP* data in the near future.

The MCMC chains we have generated are available via e-mail from the authors.

We thank M. Kaplinghat, R. Meyer and K. Ganga for useful conversations, B. Luey for some programming, B. Chaboyer for sharing results prior to publication and the Fermilab Reading Group for comments on an earlier version. LK is supported by NASA, NC by the NSF and CS by the DoE.

REFERENCES

Becker, R.H. et al., 2001, astro-ph/0108097
Bennet et al., 1996, ApJ 464, L1
Best N.G., Cowles M.K. and Vines S.K., 1995 CODA manual version 0.30 (Cambridge: MRC Biostatistics Unit)
Bond, J.R., Jaffe, A.H. & Knox, L., 2000, ApJ 533, 19
Christensen, N., Meyer, R., Knox, L. and Luey, B., 2001, Classical and Quantum Gravity, 18, 2677.
S. Dodelson and L. Knox, 2000, *Phys. Rev. Lett.* **84**, 3523.
Djorgovski, S.G., Castro, S.M., Stern, D., Mahabal, A., 2001, astro-ph/0108069
Efstathiou, G. et al., 2001, astro-ph/0109152
Efstathiou, G., 2001, astro-ph/0109151
Efstathiou, G. & Bond, J.R., 1999, MNRAS 304, 75
Eisenstein, D.J., Hu, W. & Tegmark, M., 1999, ApJ, 518, 2
Ferreras, I., Melchiorri, A. & Silk, J., 2001, MNRAS 327, L47
Freedman, W., 2001, ApJ, 553, 47
Halverson, N. et al., astro-ph/014489
Hu, W., Fukugita, M., Zaldarriaga, M., Tegmark, M., 2001, ApJ, 549, 669.
Hu, W. & White, M., 1997, ApJ, 479, 568
Kaplinghat, M., Knox, L. & Skordis, C., in preparation.
Krauss, L, & Chaboyer, B., in preparation.
A. Lee et al., astro-ph/0104459
Leitch, E. et al., astro-ph/0104488
Lewis, A., Challinor, A. & Lasenby, A., 2001, ApJ 538, 473
B. Netterfield et al., astro-ph/0104460
Perlmutter, S. et al., ApJ, 1999, 517, 565.
Perlmutter, S., Turner, M., & White, M., 1999, Phys. Rev. Lett., 83, 670
Pryke, C. et al., 2001, astro-ph/0104490
Knox, L., The Radical Compression Data Analysis Package, http://bubba.ucdavis.edu/knox/radpack.html
Riess, A. et al., 1998, AJ, 116, 1009
Seljak, U. & Zaldarriaga, M., 1996, ApJ, 469, 437
Tegmark, M., Zaldarriaga, M. & Hamilton, A.J.S., 2001, Phys. Rev. D 63, 043007
Wang, M., Tegmark, M. & Zaldarriaga, M., astro-ph/0105091

[1] *MAP*: http://map.gsfc.nasa.gov

[2] *Planck*: http://astro.estec.esa.nl/Planck/

TABLE 1

PARAMETER BOUNDS

Parameter	mean	standard deviation
ω_b	0.021	0.002
ω_d	0.145	0.021
Ω_Λ^1	0.49	0.17
$z_{\rm ri}^1$	6.0	0.14
A	6.7	0.56
n	0.96	0.04
$u_{\rm DASI}$	1.00	0.03
$u_{\rm Boom}$	1.07	0.03
$u_{\rm Maxima}$	1.00	0.03
$\rm fwhm_{Boom}^1$	13'.9	0'.3
t_0 (Gyr)	14.0	0.48
h^1	0.59	0.07
Ω_m^1	0.51	0.17
ω_Λ^1	0.19	0.11
ω_m	0.166	0.021
$c\eta_0$ (Gpc)	13.95	0.56
θ_s	35'.5	0'.43
$l_{\rm eq}$	168	15
l_d	1392	18
H_2	0.481	0.024
H_3	0.486	0.030
$t_z \times (1+z)^{3/2}$	16.0	1.0

NOTES.—The mean and standard deviations for the ten chain parameters (top) plus derived parameters (bottom). For these results we use all the data with our weakest prior assumptions. Units of A are arbitrary. See Hu et al. (2001) for the definition of $l_{\rm eq}$, l_d, H_2 and H_3. The 1 superscript indicates those parameters whose uncertainties are not well–described by a mean and standard deviation. For example, the posterior probability distribution for $z_{\rm ri}$ is not significantly different from the prior one we assumed, which is uniform between 5.8 and 6.3.